Measuring and modelling a microwave amplifier by means of the LSNA

Wendy Van Moer, Yves Rolain and Alain Barel
Vrije Universiteit Brussel (Dept. ELEC/TW); Pleinlaan 2; B-1050 Brussels (Belgium)
Phone: +32.2.629.28.68; Fax: +32.2.629.28.50; e-mail: Wendy.VanMoer@vub.ac.be

Abstract - A measurement based model for a microwave system operating in a power range up to several dB's of compression over its full operation frequency band is proposed. The measurements of the nonlinear behavior of the amplifier are performed with the Large Signal Network Analyzer. The model uses a limited amount of parameters, is easy to implement in an existing simulator, does not require the publishing of internal schematics, and predicts the response of the component over its whole working area. This model is hence a candidate for inclusion in data sheets.

I. INTRODUCTION

Classically, the response of a nonlinear device in mild compression to a Continuous Wave (CW) input is modelled using a polynomial Volterra model [1]. Nowadays, calibrated measurements of the absolute input and output waves of such a device can be performed with a Large Signal Network Analyzer (LSNA) [2]. Combining model and measurements, a polynomial model for the device response at a single frequency can be obtained. This approach is called the VIOMAP [3].

When the device is excited by a pure sine wave $X(f_1)$ (no harmonics at the input!), the fundamental output $Y(f_1)$ predicted by a VIOMAP is:

$$Y(f_1) = \sum_{n=0}^{\infty} H_{2n+1} \cdot X^{n+1}(f_1)X^n(-f_1) \qquad (1)$$

For mild compression (below 1 dB) this series can often be truncated after the second term without a significant increase of the modelling error,

$$Y(f_1) = H_1(f_1)X(f_1) + H_3(f_1, f_1, -f_1)X^2(f_1)X(-f_1) \qquad (2)$$

Herein, the complex values $H_1(f_1)$ and $H_3(f_1, f_1, -f_1)$ are the sampled values of the kernel functions $H_1(f)$ and $H_3(f_1, f_2, f_3)$ as defined in the Volterra theory [1]. Determining these complex values is sufficient to describe the device response to a sine wave at a fixed frequency.

Since measurements of the complex waves impinging the device are available, the sampled kernel values can be estimated using some kind of least squares approach.

This model models the complex output sine wave (magnitude and phase), when the complex input sine wave is given, but is only valid at 1 frequency f_1. Hence, it combines both the AM/AM and the AM/PM characteristic.

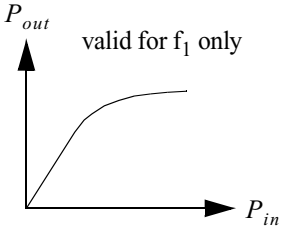

Figure 1 : Example of P_{out} vs. P_{in} at frequency f_1

Figure 1 illustrates the typical AM/AM result for a device in compression.

This model contains absolutely no information about the device behavior at different frequencies. Theoretically speaking, the measurements and the model extraction have to be done all over again if the behavior of the system is required at any other frequency (even close to f_1),.

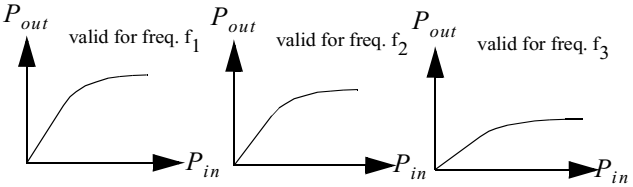

Figure 2 : Input-output relation at different frequencies

Even if the theory states that nothing can be told at frequencies different from f_1, it is reasonable in practice to assume that there is only a small difference of the system behavior for frequencies that are close to each other. Hence the VIOMAP is a smooth function of the frequency, at least in the bandwidth of the device. Measurements will show that, for a real-world component, this is indeed the case.

This smooth behavior indicates that the kernel functions H_1 and H_3 are also smooth functions of the frequency. Since these kernel functions are generalizations of a transfer function, a rational model in the complex pulsation ω is assumed to hold for these quantities.

As a result, the final model becomes a two dimensional polynomial/rational model in respectively the input spectrum and the frequency variables.

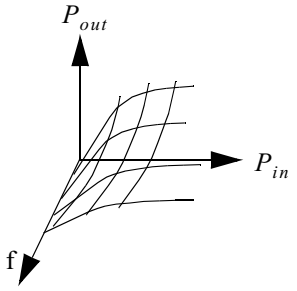

Figure 3 : P_{out} modelled as function of P_{in} and f

Once this model is known, the input-output behavior of the amplifier can be predicted for any combination of CW input power and frequency within the measured range.

II. Measuring the Nonlinear Behavior of the Amplifier

A power amplifier of type MAR6 (Mini-Circuits) will be measured and modelled. The supply voltage is set to 4V, while the device output is terminated in a 50Ω load. Absolutely calibrated incident and reflected wave spectra at both ports of the DUT are measured by the Large Signal Network Analyzer (hp85120a-k60) [2].

A. The Large Signal Network Analyzer

The LSNA is an absolute wavemeter that allows to capture the whole wave spectrum in one single take. The instrument is able to measure the absolute magnitude of the waves as well as the absolute phase relations between the harmonics. In other words, the LSNA can be seen as an absolute Fast Fourier Transform (FFT) analyser for microwaves.

Figure 1 represents a simplified block schematic of a two-port LSNA to perform connectorised CW measurements.

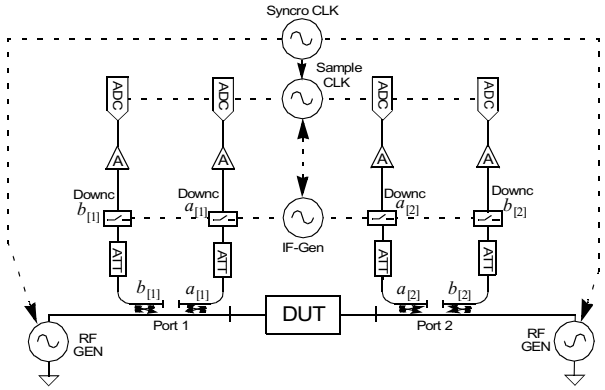

Fig. 1. Simplified block schematic of a two-port LSNA

The DUT can be excited at one or both ports by an RF generator. The incident and reflected waves at both ports of the DUT are then measured through couplers. The high frequency content of the signals does not allow to digitize these signals immediately. Therefore, the measured RF spectrum is downconverted to an IF spectrum by using harmonic mixing. This part of the setup is referred to as the downconvertor of the LSNA and is in fact the key component of the instrument: four fully synchronised RF data acquisition channels are available. After downconversion, the measured data can be amplified and digitized by four synchronised analog-to-digital convertor (ADC) cards of type HPE1437. The ADC cards sample the data at a rate of 20 MHz. The four ADC cards, the downconvertor and the RF generator are clocked by a common 10 MHz reference clock in order to obtain a fully synchronised phase coherent measurement instrument.

The calibration of a LSNA consists of three steps: a classical S-parameter calibration, a power calibration and a phase calibration. After the S-parameter calibration, the LSNA can be easily used as a classical vectorial network analyser to obtain S-parameter measurements. The power calibration is done by using a power meter, while the phase calibration is based on a known reference element which is called a 'golden diode'. The phase relations between the frequency components of the 'golden diode' signal are assumed to be exactly known. Measuring the reference signal with the LSNA and comparing the measured phase relations with the known phase relations, allows to correct the measured signals of a DUT in phase. By the additional power and phase calibration, absolute waves are obtained and nonlinear effects can be measured.

B. Measurement Results

The amplifier input is excited by a single tone. The frequency is stepped from 600 to 1500 MHz in 20 MHz steps. The input power is stepped from -20 to -8 dBm in steps of 0.2 dB. At -8 dBm, the 2 dB compression point is reached in the pass band of the device. Sample variances for the measured spectra are obtained using 5 repeated measurements.

The magnitude of the wave quotient $b_2(\omega, P)/a_1(\omega, P)$ is shown in figure(4). This nicely shows that, as is required for the model, the gain surface is a smooth surface over a wide range of powers and frequencies.

Figure 4 : Measured wave quotient b_2/a_1 as a function of the input power and frequency.

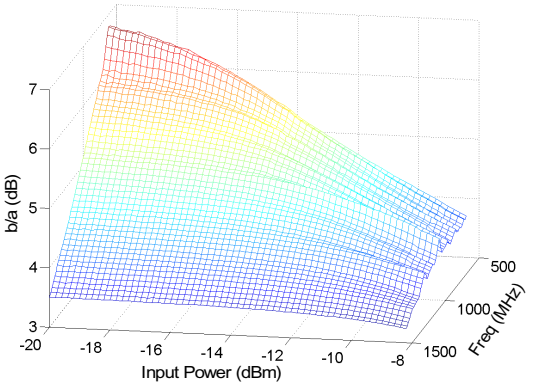

III. MODELLING THE AMPLIFIER

To extract a model for the surface describing the transport from a_1 to b_2 starting from measurements, a two step approach is used. In the first step, a different model is extracted for the power dependency of the device at each measured frequency. Here, a 7th order VIOMAP model is selected. This yields one value for the kernels H_1, H_3 H_5 and H_7 for each of the 46 measured frequencies.

In the second step, each frequency dependent quantity is modelled as a linear, time invariant system. A parametric frequency domain rational transfer function model is now estimated using a maximum-likelihood method ([4]) on each set of kernel values. 4 stable rational models of different model structure result.

Table 1: rational model structure

Kernel	degree numerator	degree denominator
K_1	4	4
K_3	10	8
K_5	10	8
K_7	9	8

The estimated kernel values at the discrete frequency set and the rational model evaluated at the same frequency set are shown for K_1 and K_5. Figure 5 shows the very close match between model and kernel values for K_1. Taking the uncertainty into account, no significant residual remains. For K_5, the situation is less clear as the apparent noise level is larger than what is expected from the measurements. This phenomenon will reappear later in the discussion and will be discussed there.

Figure 5 : Magnitude and phase of K1 and K5, Kernel values (green) and model (blue)

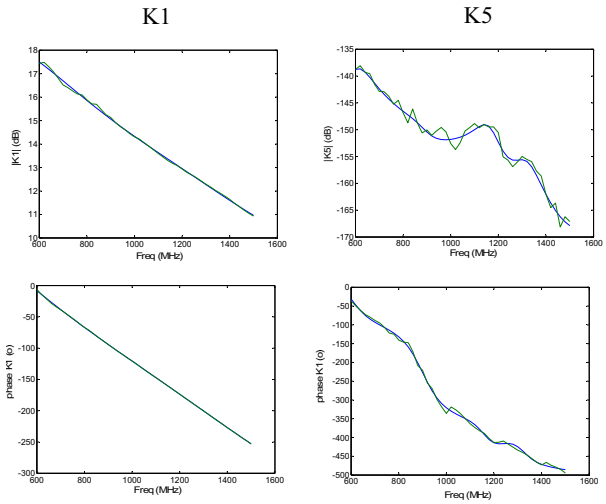

The experimental variances that were obtained by repeated measurements, are used in both steps to weight the estimator and validate the models.

After the two step procedure, the resulting model becomes:

$$b_2(f_0) = H_1(f_0)a_1(f_0) + H_3(f_0)a_1^2(f_0)a_1(-f_0) + \ldots \\ H_5(f_0)a_1^3(f_0)a_1^2(-f_0) + H_7(f_0)a_1^4(f_0)a_1^3(-f_0) \quad (3)$$

This model can easily be integrated in a simulator to describe the component, and is capable of simulation for power levels ranging from -20 dBm to -8 dBm and frequencies of 600 MHz to 1500 MHz.

To assess the quality of the model, the wave quotient that was shown in Figure 4, is now recalculated on the same power/frequency grid using the estimated model. The result is shown in Figure 6. Note the good agreement between model and measurement for the higher end of the frequency band and the power levels up to -10 dBm. For higher power levels, the differences between model and measurement start to increase. To have a quantitative view of the model quality, the magnitude of the relative complex error $(K_{model} - K_{meas})/K_{Meas}$ is shown in Figure 7. Note that the error is at least -20 dB down over all settings.

However, the shape of the error function clearly indicates that there are remaining problems in the modelling. To know if the error is mainly located in the power or the frequency modelling, the wave quotient is again calculated, but this time the kernels, as estimated in the first estimation step, are used for the surface reconstruction. Figure 8 clearly shows that this part of the estimation is the most error prone, especially when the compression level gets high, and this even if the model fit of the power characteristic is of high quality (error smaller than -20 dB).

This could be caused by harmonic effects at the input and can adequately be tackled as explained in [5]. On the other hand, it is clear that the proposed 2 step approach can at best yield a suboptimal solution, as the optimal estimates can only be reached if all the parameters are estimated together.

The proposed example shows that the rational transfer function model is capable to capture the behavior of a smooth non-linearity in a wide frequency band. The complexity of the rational models required is still acceptable and leads to fast simulations. Remember that only 1 model is required to model the fundamental component of the amplifier over a wide band of power levels and fundamental frequencies!

Extension of this model to the harmonic components of the output is quite straightforward. Since a new VIOMAP equation will result for these components, the extraction will have to be restarted, but all the required data are present in the measurements of the network analyzer.

IV. CONCLUSION

Using a Large Signal Network Analyzer, it has been shown that it is indeed possible to extract a model for the spectral output components of an amplifier operating in CW over a wide range of power levels and a wide frequency band. The model remains of acceptable complexity and is suitable for simulation purposes. As such, it is a candidate for the inclusion in the data sheet of RF amplifiers, as an extension of the IP3 and 1dB compression point.

V. REFERENCES

[1] M. Schetzen, "The Volterra and Wiener Theories of Nonlinear Systems", John Wiley & Sons, USA, 1980.

[2] T. Van den Broeck, J. Verspecht, "Calibrated Vectorial Nonlinear Network Analyser", *IEEE-MTT-S*, San-Diego, USA, 1994, pp. 1069-1072.

[3] F. Verbeyst and M. Vanden Bossche, "VIOMAP, the S-parameters Equivalent for Weakly Nonlinear RF and Microwave Devices", Transactions on Microwave Theory and Techniques, Vol. 42, Dec. 1994, pp. 2531-2535.

[4] J. Schoukens and R. Pintelon: "Frequency domain Identification: Guidelines for the practical user", Pergamon Press, 1995.

[5] P. Crama, Y. Rolain, W. Van Moer and J. Schoukens. Separation of the nonlinear source load pull from the nonlinear system behavior, *57th ARFTG Conference Digest*, Phoenix, USA, May 2001, pp. 53-58.

Figure 6 : Modelled wave quotient b_2/a_1 as a function of the input power and frequency

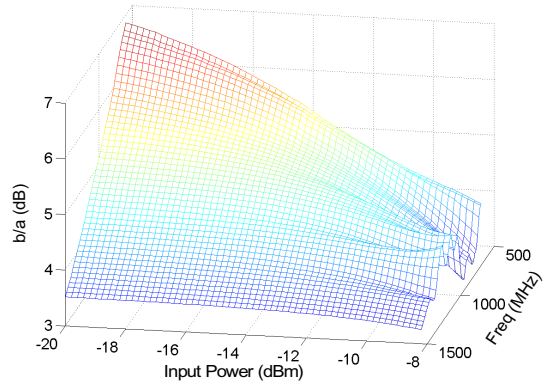

Figure 7 : Magnitude of the relative error between model and measurement as a function of input power and frequency

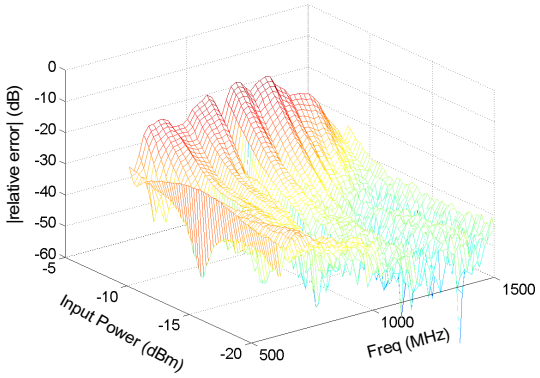

Figure 8 : Modelled wave quotient b_2/a_1 as a function of the input power and frequency